This is the accepted manuscript made available via CHORUS. The article has been published as:

Fate of a Soliton in a High Order Spatial Mode of a Multimode Fiber

A. Antikainen, L. Rishøj, B. Tai, S. Ramachandran, and G. P. Agrawal

Phys. Rev. Lett. **122**, 023901 — Published 15 January 2019

DOI: 10.1103/PhysRevLett.122.023901

The fate of a soliton in a high order spatial mode of a multimode fiber

A. Antikainen,[1,*] L. Rishøj,[2] B. Tai,[2] S. Ramachandran,[2] and G. P. Agrawal[1]

[1] *The Institute of Optics, University of Rochester, Rochester, NY 14627, USA*
[2] *Department of Electrical Engineering, Boston University, Boston, MA 02215, USA*

(Dated: October 29, 2018)

We show numerically that under certain conditions noise-induced soliton self-mode conversion dominates over soliton self-frequency shift for a soliton in a high order spatial mode of a multimode optical fiber. The input soliton has to be group index matched to a lower-order mode for a frequency separation for which the Raman gain is non-negligible, and this condition determines the wavelength of the pulse growing from noise. The phenomenon has no known analogues in single-mode or graded-index fibers. The results demonstrate that it is possible for a noise-induced physical process to dominate over a seeded one even for noise levels at the fundamental limit.

Raman scattering of light in single-mode optical fibers is a well understood effect [1]. It leads to energy transfer to lower frequencies determined by the lattice vibrations of the medium. For fused silica the Raman gain spectrum peaks at a frequency separation of approximately 13 THz, which dictates the frequencies of the inelastically scattered photons in optical fibers [2]. A nanosecond scale pulse can generate a Stokes pulse at a longer wavelength through Raman-induced energy transfer. The Stokes pulse then seeds the process leading to stimulated Raman scattering. However, since the two pulses are separated by roughly 13 THz, they generally have very different group velocities and become separated in time and the energy transfer stops [1]. For short pulses (< 10 ps) the walkoff occurs so fast that Stokes pulses cannot be observed. For even shorter pulses (< 1 ps) the red part of the wide spectrum seeds the Raman process and energy is transferred from the blue side to the red side. Such intrapulse Raman scattering is responsible for the well-known soliton self-frequency shift (SSFS) [3].

Solitons in graded-index multimode fibers have been studied in recent years and they experience the same effects as their single-mode counterparts with additional intermodal interactions [4–7]. Even though graded-index multimode fibers can support very rich soliton propagation dynamics, they resemble single-mode fibers in the sense that the group velocities of the modes are very similar by design. Because of this, Raman-induced Stokes pulse generation behaves in a similar manner compared to single-mode fibers [8, 9].

The situation changes in other types of fibers, such as step-index fibers, where the group velocities for different spatial modes vary considerably. In such fibers two spectrally separated pulses in different modes can copropagate at the same group velocity. Through careful selection of the modes and the central frequencies of the pulses, the frequency separation required for group velocity matching can be made to coincide with the Raman gain peak near 13 THz. It was recently demonstrated experimentally [10, 11] that under such conditions energy can indeed be efficiently transferred from one mode to another through intermodal Raman scattering when solitons are launched into a high order mode of a step-index multimode fiber. The process is referred to as soliton self-mode conversion (SSMC) [11], and the experiments showed nearly complete energy transfer between different spatial modes. It was also shown recently that numerical solutions to the coupled-mode generalized nonlinear Schrödinger equation [12] are able to qualitatively replicate the experimental results [13].

In this Letter we demonstrate that SSMC, which is a noise-seeded process, always eventually dominates over the seeded SSFS process even for ultrashort (10 fs) solitons under certain conditions, one of them being group velocity matching for a frequency separation near the Raman gain peak. We also show that SSMC occurs over shorter distances for shorter solitons meaning that similar scaling laws that govern SSFS in single-mode fibers are generally true for intermodal Raman-induced interactions as well.

To model light propagation in multimode fibers we use the multimode generalized nonlinear Schrödinger equation as presented by Poletti and Horak [12]:

$$\frac{\partial A_p(z,t)}{\partial z} = i(\beta_0^{(p)} - \beta_0)A_p(z,t) - (\beta_1^{(p)} - \beta_1)\frac{\partial A_p(z,t)}{\partial t} + i\sum_{n\geq 2}\frac{\beta_n^{(p)}}{n!}\left(i\frac{\partial}{\partial t}\right)^n A_p(z,t) + i\frac{n_2\omega_0}{c}\left[1 + i\tau_s\frac{\partial}{\partial t}\right]\sum_{l,m,n} Q_{plmn}$$
$$\times\left(2A_l(z,t)\left\{R(t) * [A_m(z,t)A_n^*(z,t)]\right\} + A_l^*(z,t)\left\{\left[R(t)e^{2i\omega_0 t}\right] * [A_m(z,t)A_n(z,t)]\right\}\right), \quad (1)$$

where $A_p(z,t)$ is the temporal envelope of the p^{th} mode at the carrier frequency ω_0, β's are the dispersion param-

eters at ω_0, n_2 is the nonlinear refractive index, $\tau_s = 1/\omega_0$ is the shock time scale, $R(t) = (1-f_R)\delta(t)+1.5f_R h(t)$ is the nonlinear response function with $f_R = 0.18$ and h_R given by the experimental Raman response function [2]. The nonlinear overlap factors Q_{plmn} are defined as

$$Q_{plmn} = \frac{\varepsilon_0^2 n_0^2 c^2}{12} \frac{\int dxdy[\mathbf{F}_p \cdot \mathbf{F}_l][\mathbf{F}_m \cdot \mathbf{F}_n]}{N_p N_l N_m N_n}, \qquad (2)$$

where

$$N_k = \left[\frac{n_{\text{eff}}\varepsilon_0 c}{2} \int dxdy \mathbf{F}_k(x,y) \cdot \mathbf{F}_k(x,y))^2\right]^{\frac{1}{2}} \qquad (3)$$

and $\mathbf{F}_k(x,y)$ is the transverse field profile of the k^{th} mode. Note that we have assumed that the field profiles $\mathbf{F}_k$ are real and that the overlap factors Q_{plmn} are not dependent on frequency. As noted in [12], these simplifying assumptions can be made without compromising the generality of the results.

The step-index fiber in our simulations corresponds to the fiber used in [11] with a core diameter of 87 μm and refractive indices of $n_{\text{core}} = 1.4785$ and $n_{\text{clad}} = 1.4394$ at a wavelength of 1045 nm. The simulations included three transverse modes: the fully rotationally symmetric $\text{LP}_{0,19}$ and $\text{LP}_{0,18}$, and the anti-symmetric $\text{LP}_{1,18}$. Their transverse spatial profiles and refractive indices as a function of wavelength were determined numerically. These modes were chosen because their group indices n_g satisfy $n_g^{\text{LP}_{0,18}}(\omega_0 + 2\Delta\omega) \approx n_g^{\text{LP}_{1,18}}(\omega_0 + \Delta\omega) \approx n_g^{\text{LP}_{0,19}}(\omega_0)$ when the angular frequency ω_0 corresponds to a wavelength in the $1.1-1.6$ μm range and the separation $\Delta\omega$ is between 5 and 10 THz. The input pulse was a fundamental soliton in the $\text{LP}_{0,19}$ mode with a central wavelength of 1100 nm. The temporal full width at half-maximum (FWHM) of the soliton was varied between 10 and 80 fs. The shortest soliton is 3 optical cycles in duration but the model used here is valid down to the single-cycle regime as it does not assume a slowly-varying envelope, as was pointed out by Brabec and Krausz [14]. The nonlinear refractive index in Eq. (1) was $n_2 = 3.2\cdot10^{-20}$ m^2/W. Noise was included by adding 1 photon per longitudinal mode (frequency bin) in each spatial mode at the input end, corresponding to the fundamental limit of quantum shot noise for the $\text{LP}_{0,19}$ mode and representing a single photon at each discrete frequency in the other two modes. In practice, spontaneous Raman scattering and linear mode coupling from $\text{LP}_{0,19}$ would distribute a portion of the photons to each mode even if no power was launched in $\text{LP}_{1,18}$ and $\text{LP}_{0,18}$.

Figure 1 shows the simulated spectral evolution of solitons with input durations (FWHM) of (a) 80 fs and (b) 40 fs. Both solitons evolve in a similar manner but in different parts of the spectrum and over different length scales. The solitons undergo rapid SSFS until they transfer their energy to the $\text{LP}_{0,18}$ mode. Note that there are no temporal oscillations of the total power during the power transfer since the interacting pulses, though separated in the spectrum, are in different spatial modes that are orthogonal to one another (even when polarized along the same direction). The total temporal intensity profile is sech-shaped throughout the process. The shorter soliton shown in Fig. 1(b) experiences faster red shift and reaches longer wavelengths before energy is transferred to $\text{LP}_{0,18}$. In either case virtually no energy is transferred to the asymmetric $\text{LP}_{1,18}$ mode, and nearly 100% of all the energy (aside from the pump remnants) ends up in $\text{LP}_{0,18}$. The rapid red shift of the 40 fs soliton raises the question whether SSFS can dominate over SSMC for even shorter pulses. Figure 2 that shows the spectral evolution of a 15 fs soliton launched in $\text{LP}_{0,19}$ indicates that this is not the case.

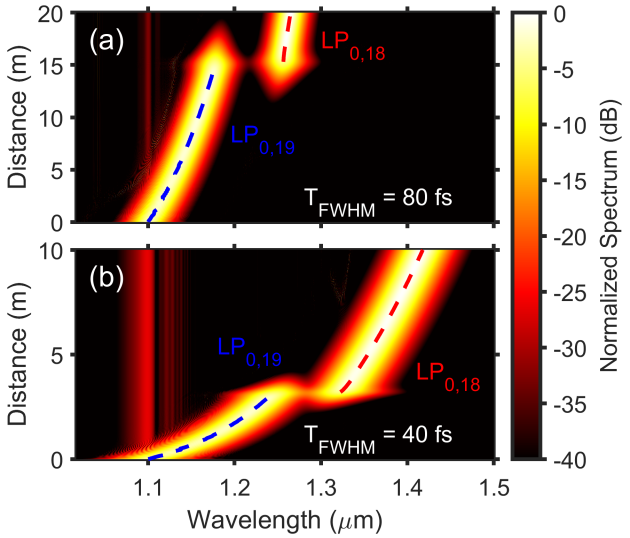

FIG. 1. The spectral evolution of a soliton with an input duration of (a) 80 fs and (b) 40 fs in the multimode step-index fiber. The spatial modes have been indicated by the dashed lines that follow the respective spectral maxima. Note the different length scales in (a) and (b).

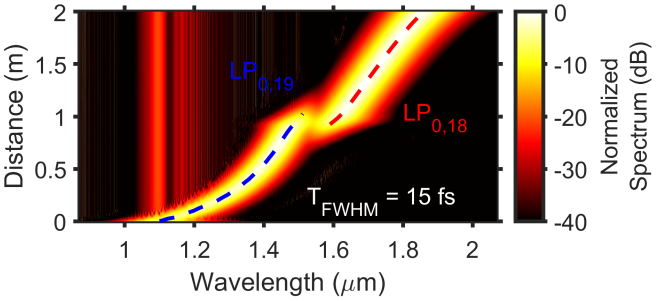

FIG. 2. The spectral evolution of a soliton with an input duration of 15 fs.

The 15 fs soliton shown in Fig. 2 red shifts even further than the solitons shown in Fig. 1 but its eventual fate is

the same: almost all the energy aside from pump remnants is transferred to $LP_{0,18}$. Such near-complete energy transfer was observed in all of the simulations regardless of the input pulse duration, which is remarkable given that short pulses red shift very rapidly and especially because the pulse on $LP_{0,18}$ grows from low-intensity noise. In reality there would also be more modes beyond the $LP_{0,18}$ mode and the process would keep on cascading [11]. These modes, such as $LP_{0,17}$, were left out of the simulations in the interest of computational simplicity.

Comparing Figs. 1 and 2 shows that the central wavelengths of the pulses during the energy transfer can be very different depending on the input soliton duration. The central wavelength of the 80 fs soliton in Fig. 1(a) is 1150 nm at the start of the energy transfer whereas Fig. 2 seems to indicate that the 15 fs soliton reaches 1.4 μm. To explain what dictates the start of the intermodal energy transfer, it is informative to look at the wavelengths of the participating pair of pulses at the onset of the process.

Figure 3 shows the frequency separation $\Delta\nu$ between the red shifting input soliton in $LP_{0,19}$ and the forming soliton in $LP_{0,18}$ at various stages of the energy transfer as a function of the central wavelength of the pulse in the input $LP_{0,19}$ mode. The blue crosses show the frequency separation at the beginning of the energy transfer which is taken to mean the point at which 1% of the total energy has been transferred from $LP_{0,19}$ to the other two modes. The red circles correspond to the stage at which exactly half of the total energy is in $LP_{0,19}$. As was seen in Figs. 1 and 2, the wavelength of the soliton in $LP_{0,19}$ during the energy transfer depends heavily on the input soliton duration. Figure 3 then shows that the frequency separation between the red shifting soliton in $LP_{0,19}$ and the pulse growing from noise in $LP_{0,18}$ depends on the $LP_{0,19}$ pulse wavelength and that this dependence very closely follows the group-velocity matching condition between $LP_{0,19}$ and $LP_{0,18}$. The fact that both the circles and the crosses fall on the group velocity matching curve indicates that the group velocity matching condition is satisfied throughout the energy transfer process. The reasons why the red circles are slightly below the curve are that during the first half of the energy transfer the soliton in $LP_{0,19}$ red shifts faster than the one forming in $LP_{0,18}$ and the blue side of the $LP_{0,18}$ pulse has experienced gain for a longer time compared to its red side due to the red shifting $LP_{0,19}$ pulse being on the blue side of the $LP_{0,18}$ pulse. We also performed the same simulations with 30 dB more noise (1000 photons per longitudinal mode in each spatial mode) and saw that the energy transfer process still closely followed the group velocity matching curve with some deviations (< 1 THz).

In general, longer input solitons have shorter wavelengths during the energy transfer, but none of the solitons studied here experienced energy transfer until they had red shifted to at least 1.14 μm. As Fig. 3 shows, the

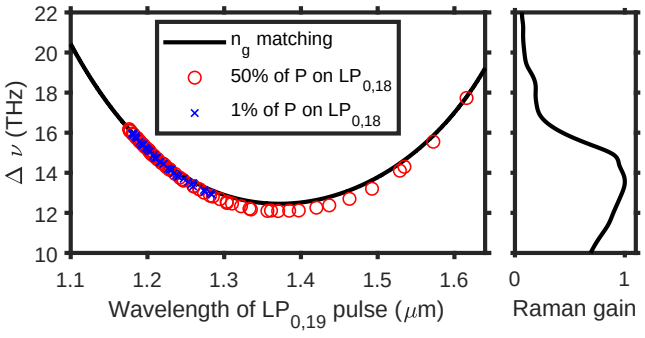

FIG. 3. The frequency separation needed to group velocity match $LP_{0,19}$ to a lower frequency in $LP_{0,18}$ as a function of the $LP_{0,19}$ soliton wavelength (solid black line). The blue crosses correspond to the stages of energy transfer in the simulations where 1% of the total energy has been transferred from $LP_{0,19}$ to $LP_{0,18}$. The red circles correspond to 50% energy transfer for the same simulations. The normalized Raman gain is shown on the right.

energy transfer requires group velocity matching and the frequency separation needed for it is 18 THz when the $LP_{0,19}$ pulse wavelength is 1.14 μm. The Raman gain is quite small for such large frequency separations (see the Raman gain curve in Fig. 3) and hence energy transfer cannot take place efficiently and the input soliton has to red shift further first to be group velocity matched to $LP_{0,18}$ for smaller frequency separations for which the Raman gain is larger.

Due to the dispersion profiles of the fiber, the frequency separation required for group velocity matching attains its minimum value of 12.5 THz when the $LP_{0,19}$ soliton wavelength is 1375 nm. For longer wavelengths the group velocity matching requires larger frequency separations again. Input solitons of all durations were observed to start the energy transfer when their central frequency reached 1.14 μm, but this energy transfer is very slow at first because it is induced by a noise floor $60 - 80$ dB below the soliton spectrum and because Raman gain is still small for a separation of 18 THz. The soliton in $LP_{0,19}$ will continue to red shift during the energy transfer process at a rate determined by its duration. The rightmost red circles in Fig. 3 correspond to the shortest input pulses and some of them have red shifted to wavelengths longer than 1.5 μm by the midpoint of the energy transfer. It is remarkable how well the process is characterized by the group velocity matching condition even for the shortest input pulses and that the two pulses stay group velocity matched throughout. It should be mentioned that the 15 fs soliton shown in Fig. 2 seems to have red shifted to ~ 1.4 μm before the energy transfer starts, but this is an illusion. The energy transfer does indeed start after the input soliton reaches 1.14 μm but by the time a certain frequency band in $LP_{0,18}$ begins to experience gain and power buildup, the input soliton has

shifted further to the red and is group velocity matched to a different frequency band (and also overlapping the spectrum of the forming pulse in $LP_{0,18}$). Thus, the initially amplified frequencies in $LP_{0,18}$ experience gain only over a short distance. Furthermore, because the spectrum of a short soliton is broad, different parts of it will amplify different frequencies in the $LP_{0,18}$ mode. The power buildup thus covers a broader frequency band and the energy is more spread out in the spectrum.

No significant power buildup was observed in the $LP_{1,18}$ mode in any of the simulations even though this mode is group velocity matched to $LP_{0,19}$ for smaller frequency separations for which Raman gain is non-negligible. For example, the input soliton at 1100 nm is group velocity matched to $LP_{1,18}$ for a frequency separation of 10 THz but yet no pulses grow in $LP_{1,18}$. There are at least two possible explanations for this. First, $LP_{1,18}$ is antisymmetric while $LP_{0,19}$ and $LP_{0,18}$ are fully rotationally symmetric, and thus a lot of the nonlinear overlap integrals given in Eq. (2) are small or identically zero. One is then inclined to think that $LP_{0,19}$ cannot couple to $LP_{1,18}$ as efficiently because of this. Second, $LP_{1,18}$ could be an intermediate step in the process and whatever energy is transferred to $LP_{1,18}$ could be immediately transferred further to $LP_{0,18}$.

To see whether $LP_{1,18}$ is an intermediate step, we performed the same set of simulations with the $LP_{1,18}$ mode completely removed. The evolutions of the solitons were almost completely identical regardless of the possibility of energy transfer to $LP_{1,18}$. This showed that the energy transfer from $LP_{0,19}$ to $LP_{0,18}$ is direct and not cascaded. The lack of power in $LP_{1,18}$ is therefore due to the smaller nonlinear overlap integrals that hinder the nonlinear interactions between $LP_{0,19}$ and $LP_{1,18}$. Note that energy transfer to $LP_{1,18}$ is still possible but transfer to $LP_{0,18}$ is dominant. In general, the efficiency of energy transfer to a certain mode is a heavily nonlinear function of group velocity matching, Raman gain, the strength of the nonlinear coupling as determined by the overlap integrals and soliton power, and any possible pre-existing power or seed in the receiving mode.

Next we briefly discuss the distance at which the energy transfer starts and the distance over which is lasts: the interaction distance. Figures 1 and 2 indicate that the energy transfer takes place closer to the beginning of the fiber and also that it occurs over a shorter distance for shorter pulses. Figure 4(a) shows the distance at which 50% of the total energy has been transferred from $LP_{0,19}$ to the other modes and the interaction length. By interaction length we mean the distance it takes for the relative energy in $LP_{0,18}$ to rise from 5% to 95%. Figure 4(b) shows the relative energy in $LP_{0,18}$ as a function of input pulse duration and propagation distance.

Figure 4(a) illustrates that the distance at which energy transfer takes place and the distance it takes for it to complete are both smaller for shorter input pulses. The

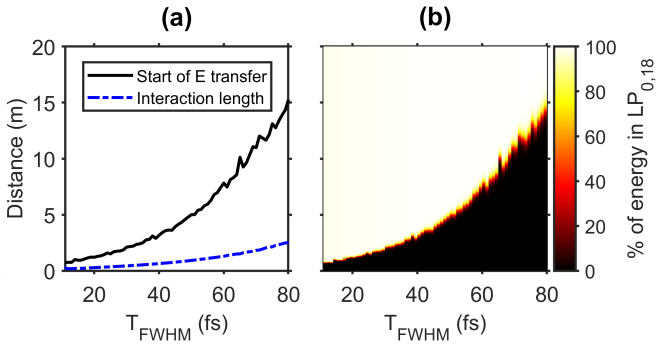

FIG. 4. (a) The distance of 50% energy transfer (solid black curve) and the interaction length (dashed blue curve) as a function of the input soliton FWHM duration. (b) The percentage of energy in the $LP_{0,19}$ mode (color coded) as a function of input soliton duration and propagation distance.

explanation for this is that the input pulses were all solitons and the high peak powers of short solitons enhance nonlinear effects. This is well known in the context of SSFS for which the rate of red shift depends inversely on the fourth power of the pulse duration [1]. Our results indicate that similar scaling laws are true for the intermodal nonlinear process of SSMC as well: SSMC occurs over shorter distances for shorter pulses. Figure 4(b) shows how nearly 100% of the initial energy ends up in $LP_{0,18}$ for all input pulse durations. It should be reiterated that losses were neglected and the dispersion was anomalous for all modes in the whole spectral window. Should there be a zero-dispersion wavelength or a zero-nonlinearity wavelength on the red side of the soliton, the soliton could transfer its energy to a dispersive wave in the non-solitonic spectral region and die out without undergoing SSFS or SSMC [15]. We therefore conclude that SSMC dominates over SSFS far from the normal dispersion regime unless the group velocity matching of the input pulse to a different mode requires large frequency separations (at least > 18 THz in silica fibers) for which the Raman gain is very small. The findings demonstrate that not only is it possible for a noise-induced process to overpower a seeded one, it can even be the norm in certain cases.

In conclusion, we numerically studied the newly-discovered phenomenon of soliton self-mode conversion (SSMC) in a step-index multimode fiber where a soliton in a high order spatial mode sculpts another soliton in a lower-order mode out of noise and trasfers all of its energy to it. The frequency difference between the two solitons during the energy transfer process was demonstrated to be accurately determined by the group velocity matching condition between the participating modes. Noise-seeded SSMC always dominated over the stimulated Raman effect of soliton self-frequency shift even for ultrashort (10 fs) solitons and in fact SSMC occurs over

shorter distances the shorter the soliton is. Notably, only one photon per longitudinal mode was enough noise for SSMC to overpower the seeded Raman effects. As a final remark we emphasize that SSMC is not specific to step-index fibers. It is a universal phenomenon and could be observed in any multimode fiber that has nonlinearly interacting modes with suitably different group velocities.

* aku.antikainen@rochester.edu

[1] G. P. Agrawal, *Nonlinear Fiber Optics*, 5th ed. (Academic, 2013)

[2] R. H. Stolen, J. P. Gordon, W. J. Tomlinson, and H. A. Haus, J. Opt. Soc. Am. B **6**(6), 1159–1166 (1989)

[3] F. M. Mitschke and L. F. Mollenauer, Opt. Lett. **11**, 659–661 (1986)

[4] W. H. Renninger and F. W. Wise, Nat. Commun. **4** 1719 (2013)

[5] L. G. Wright, W. H. Renninger, D. N. Christodoulides, and F. W. Wise, Opt. Express **23**, 3492–3506 (2015)

[6] K. Krupa, A. Tonello, B. M. Shalaby, M. Fabert, A. Barthélémy, G. Millot, S. Wabnitz, and V. Couderc, Nat. Photon. **11**, 237–241 (2017)

[7] A. S. Ahsan and G. P. Agrawal, Opt. Lett. **43**(14), 3345–3348 (2018)

[8] K. S. Chiang, Opt. Lett. **17**(5), 352–354 (1992)

[9] H. Pourbeyram, G. P. Agrawal, and A. Mafi, Appl. Phys. Lett. **102**, 201107 (2013)

[10] L. Rishøj, B. Tai, P. Kristensen, and S. Ramachandran, Laser Congress, ATh1A.6 (2016)

[11] L. Rishøj, B. Tai, P. Kristensen, and S. Ramachandran, arXiv:1805.06037

[12] F. Poletti and P. Horak, J. Opt. Soc. Am. B **25**, 1645–1654 (2008)

[13] A. Antikainen, B. Tai, L. Rishøj, S. Ramachandran, and G. P. Agrawal, Conference on Lasers and Electro-Optics, FTh4E.3 (2018)

[14] T. Brabec and F. Krausz, Phys. Rev. Lett. **78**(17), 3282–3285

[15] F.R. Arteaga-Sierra, A. Antikainen, and G. P. Agrawal, Phys. Rev. A **98**(1), 013830 (2018)